JOURNAL OF GEOPHYSICAL RESEARCH, VOL. 103, NO. D9, PAGES 10,817–10,825, MAY 20, 1998

A Lagrangian estimate of aircraft effluent lifetime

M. R. Schoeberl and C. H. Jackman
NASA Goddard Space Flight Center, Greenbelt, Maryland

J. E. Rosenfield
General Sciences Corporation, Laurel, Maryland

Abstract. The lifetime of aircraft exhaust is estimated using multiyear diabatic trajectory integrations using United Kingdom Meteorological Office and Goddard Space Flight Center (GSFC) Data Assimilation Office winds. Instantaneous January trajectory parcel releases in the midlatitude stratosphere at 19, 16, 14, 13, and 11 km are compared. The first two cases correspond to the proposed flight altitudes of high-speed supersonic aircraft. The last two cases correspond to subsonic flight altitudes. Parcels descending below 250 hPa are eliminated as would occur when aircraft effluent reaches the troposphere. After a transient adjustment period the total number of parcels in most experiments decays exponentially with a decay period (lifetime) of about 1 year. This is the lifetime of the longest-lived eigenmode as discussed by *Prather* [1996]. Our 1-year lifetime is shorter than the 1.5 year GSFC two-dimensional (2-D) model lifetime for the same release, but in good agreement with the 1.13 year GSFC 3-D model lifetime. We also find that the effluent lifetime is slightly longer in the southern hemisphere midlatitude stratosphere than in the northern. Both the 13 and 11 km releases are mostly within the stratospheric middle world and rapidly leave the stratosphere. We conclude that there will be a small impact of subsonic aircraft exhaust on the larger stratosphere. Finally, we find that our overall lifetime results are fairly sensitive to the lower stratospheric heating rates.

1. Introduction

One of the major uncertainties in the assessment of the fate of the long-lived components of pollution from stratospheric aircraft (e.g., NO_y and H_2O) is the transport of effluent from the emission regions. Transport controls the global lifetime of effluent as well as distribution of effluent to regions outside the aircraft corridors. A series of studies have already been performed to examine effluent transport using two-dimensional (2-D), three-dimensional (3-D), and trajectory (or Lagrangian) models. These studies have been reviewed in a number of papers and reports and are summarized by *NASA* [1995] and by *Weaver et al.* [1996]. An important issue emerging from these studies is the relevance of tropical lofting and its impact on the overall lifetime of the effluent in the stratosphere. The lofting of the aircraft exhaust will increase the stratospheric residence time and would also increase the ozone destruction due to exhaust through the catalytic cycles involving NO_y.

Plumb [1996], among others, has pointed out that if aircraft NO_y could be advected into the tropics and lofted to higher altitudes, the increase in NO_y would then lead to an increase in nitrogen radicals (NO_x) which would greatly enhance stratospheric ozone loss. Whether this can happen or not is determined by the degree of tropical isolation and magnitude of the vertical motion in the tropics. *Avallone and Prather* [1996], *Minschwaner et al.* [1996], and *Volk et al.* [1996] have argued from observations that the lower tropical stratospheric air is up to 50% diluted by midlatitude air. They estimated a time scale for tropical-midlatitude mixing of 13 months. Above 20 km, *Schoeberl et al.* [1997] have argued from Upper Atmosphere Research Satellite (UARS) data that the tropical-midlatitude exchange time is 18 months or longer.

An issue not receiving as much attention as the tropical lofting of supersonic aircraft pollutants is the impact of subsonic aircraft pollutants. There is a significant amount of subsonic exhaust already being emitted into the stratosphere. However, subsonic aircraft fly within the very lowest part of the midlatitude stratosphere. Subsonic aircraft rarely cross the 385 K isentrope which defines the boundary between the "middle world" (the region above the midlatitude tropopause and below the isentrope touching the tropical tropopause, roughly 385 K), and the "overworld" (the region above 385 K) [see *Holton et al.*, 1995]. Both diabatic heating rate calculations and mass balance suggest that most of the material in the middle world will soon exit the stratosphere. Thus most subsonic aircraft exhaust is probably flushed quickly from the stratosphere, but given the large amount of this exhaust, if even a fraction could enter the overworld stratosphere the chemical impact may be significant.

The chemical lifetime of a gas (sometimes called residence time) is usually defined as the total amount of a species divided by production rate after steady state is reached. This assumes that the loss rate (L) has a global functional form: $L = -\mu/l$ where μ is the gas mixing ratio and l is lifetime. For aircraft exhaust experiments the pollutant lifetime is often computed after a long (e.g., 5 year) continuous release so that the model transients have died down. Using the trajectory model [*Schoeberl and Sparling*, 1995], we use an alternative method which is more computationally expedient. We perform a single pulse release and look for the period where the decrease in the number of parcels can be well characterized as an exponential form. The time rate of change of the $\log_e$ of the parcel number

Paper number 98JD00363.
0148-0227/98/98JD-00363$09.00

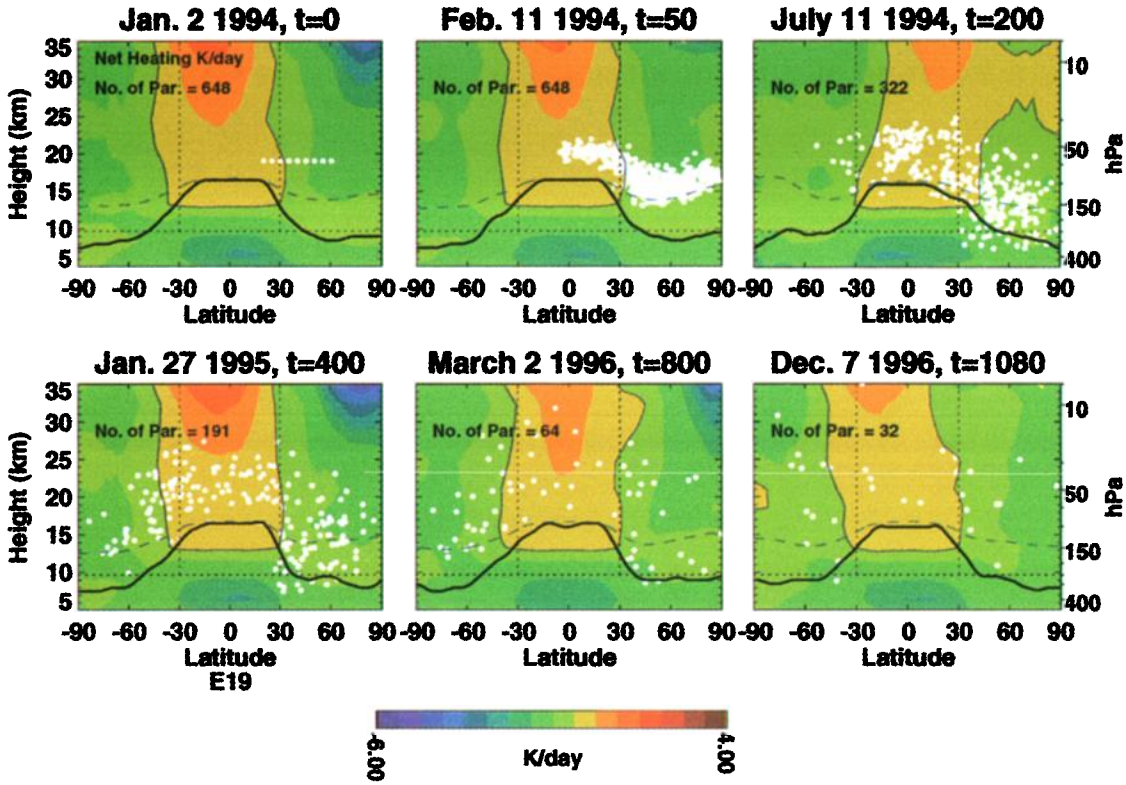

Plate 1. A series of six snapshots from experiment E19. Each panel shows the parcels as white circles superimposed upon the zonal mean net heating rate in K/day. The thick black line is the zonal mean tropopause, while the black dashed line is the zonal mean 385 K contour. The total number of parcels is indicated in the upper corner of each panel. The heating rate colored surfaces are spaced at 0.5 K/day with the thin black line dividing positive from negative. The horizontal dotted line shows the removal altitude (250 hPa); the vertical dotted lines show 30°N and 30°S latitudes. The altitude is log pressure height in km ($7 \log_e (1000./p)$ where p is the pressure in hectopascals).

within the exponential decay regime is then approximately the inverse lifetime. This method is computationally faster than the run-to–steady state approach because the CPU requirements for the trajectory model are proportional to the number of parcels.

The run-to–steady state estimate of lifetime and the pulse-decay release estimate of the lifetime do not necessarily give the same number, although they are usually quite close. The explanation for this discrepancy was discovered by *Prather* [1996]. He noted that the response to the emission of a trace gas can be described as the excitation of eigenmodes whose eigenvalues correspond the trace gas growth and decay rates. If the source of the trace gas is removed (but not the sink), then trace gas amount exponentially decays with time. The slope of the long decay tail in the constituent amount is determined by the eigenvalue of the most long-lived eigenmode. The lifetime of the long-lived mode is usually longer than the steady state estimate for the lifetime, because the steady state lifetime estimate includes the shorter lifetimes of other modes excited by the steady state forcing [*Prather*, 1996]. The forced modes dominate the system at steady state since the transient modes have died out. However, the longest-lived mode is usually the dominant forced mode at steady state because only a small projection of the forcing on this modes is required to maintain it. Thus the difference between the steady state lifetime and the lifetime of the longest-lived mode is usually not large, as will be shown for one of our experiments.

Global lifetime estimates for aircraft exhaust made by 2-D models using the run-to–steady state method vary from 1 to 3 years, with most models clustering near 1.5–2 years for the first year [*NASA*, 1993]. The Goddard Space Flight Center (GSFC) 2-D model with improved dynamics [*Jackman et al.*, 1996] using the pulse-decay method gives a lifetime of 1.5 years; with the old dynamics scheme the reported run-to–steady state lifetime was 1.7 years. However, more relevant to this study is the run-to–steady state 3-D model lifetime estimate made by *Weaver et al.* [1996]. For a 19 km (Mach 2.4) scenario the 3-D chemical transport model using Goddard Earth Observing System (version 1, GEOS-1) winds gives an emission lifetime of 1.15 years. The shorter effluent lifetime for the 3-D model compared to the 2-D models may be due to stronger midlatitude stratosphere-troposphere (ST) exchange in the 3-D models compared to the 2-D models, or may be due to greater eddy mixing out of the tropical stratosphere into the midlatitudes where material leaves the stratosphere [*Weaver et al.*, 1996].

The trajectory experiments described below can be compared to the results of the 3-D and 2-D model calculations and provide some insight into the differences between the 2-D and 3-D results. Although the trajectory model is three dimensional, we move parcels across isentropic surfaces using the net diabatic heating rates rather than using the kinematic vertical velocity as is used in the 3-D chemical model. Diabatic vertical velocities are used in the 2-D models.

The next section describes the model configuration and input data sets. Section 3 discusses our experimental results, and section 4 summarizes our findings.

Table 1. Parcel Statistics

Experiment	Initial Delta, %	Global Lifetime	NH Lifetime	SH Lifetime	Tropical Lifetime	Comment
E19	55%	1.0	0.81	1.3	1.1	19 km NH release, UKMO winds
E19M	55%	1.1	0.86	1.3	1.3	7380 parcels
E19D	80%	1.2	0.87	1.3	2.5	STRAT data instead of UKMO
E19C	...	0.93	...	...	...	continuous release
E190	35%	1.6	0.9	3.1	2.7	diabatic heating unchanged
E16	65%	1.0	0.5	1.1	1.0	16 km release
E14	80%	0.86	0.43	0.68	0.93	14 km release
E13	95%	0.95	...	...	...	13 km release
E11	100%	0.05	...	...	...	11 km release
^{14}C-520 K	30%	1.3	1.4	5.4	1.5	bomb release

The experiment number is the release altitude (E19 = 19 km release); see text for further experiment descriptions. All releases are in zonal bands from 20°–60°N with globally balanced heating rates except E190. NH is from 90°N to 30°N, tropics is from 30°N to 30°S, and SH is from 90°S to 30°S. Units are years except where indicated. Initial delta refers to the rapid initial drop of total parcel number in percent. This is followed by the slower exponential decrease from which the lifetime is computed. In the E11 experiment the initial delta describes the entire experiment, so the lifetime refers to an exponential fit to the initial delta.

2. The Trajectory Model and Experiment Scenarios

For almost all of our experiments the air parcel trajectories were computed using wind data from the United Kingdom Meteorological Office (hereafter UKMO) assimilation system [*Swinbank and O'Neill*, 1994a]. The UKMO assimilation winds are closer to observations than balanced winds in the tropics, and the UKMO system generates a tropical quasi-biennial oscillation [*Swinbank and O'Neill*, 1994b]. The net heating and cooling rates, which are not provided as part of the UKMO analysis, are derived from the UKMO temperatures using monthly mean and zonal mean ozone distributions and climatological cloud fields [*Rosenfield et al.*, 1994, 1997]. The use of zonal mean ozone fields instead of 3-D fields does not significantly change our results, since the trajectory parcels see the time-integrated effect of the heating and cooling in their rapid zonal motion.

UKMO winds were used for most of the 3-year experiments instead of Goddard Data Assimilation Office (DAO) winds used by *Weaver et al.* [1996] because diabatic heating rates for DAO's GEOS-1 or GEOS-STRAT assimilations were not available. After most of the UKMO experiments were performed, 1 year of GEOS-STRAT data (October 1995 to October 1996) with diabatic heating rates became available. The E19 experiment (discussed below) was repeated using the GEOS-STRAT data by recycling the winds after 12 months. UKMO provides a once daily analysis, while the GEOS-STRAT system provides an analysis every 6 hours.

We also compare our E19 trajectory calculation (described below) to an experiment run with the Goddard 2-D model of *Jackman et al.* [1996]. The 2-D model diabatic heating rate code uses the same climatological ozone and cloud fields as used with the UKMO data, but National Center for Environmental Prediction (NCEP) climatological temperatures are used instead of UKMO temperatures. The differences between the NCEP, GEOS-STRAT, and UKMO temperature data sets are small, and the computed heating rates are equivalent.

To insure global conservation of mass, and to generate results consistent with the 2-D and 3-D models, the global mean net heating rate is computed for each pressure level above 100 hPa and is uniformly subtracted from the heating rate at that level to insure that the net global mean heating is zero. This procedure was first used by *Murgatroyd and Singleton* [1961] and was more recently discussed by *Shine* [1989] and *Olaguer et al.* [1992]. Olaguer et al. advocated constraining the isentropically averaged global heating rate, which appears to produce better results above 30 km. Below 30 km the pressure and potential temperature averaging procedures produce similar discrepancies. As pointed out by both Olaguer et al. and Shine, it is not clear that uniformly adjusting the net heating rates is the correct method for dealing with nonzero globally averaged net heating, but this is the best assumption we can make given no additional information on the source of the discrepancy. Aside from the issue of net global heating, another reason for making adjustments to the diabatic heating rate is to determine the sensitivity of the calculation to the uncertainty in the heating rates.

For our effluent studies, parcels are released instantaneously on a regular grid in the northern hemisphere (NH). Parcels are spaced every 5° in latitude and 5° in longitude from 20°N to 60°N; 642 parcels are released. The release distribution is based upon the projected zonal mean release scenarios reported by *NASA* [1995, Figure 17] and is equivalent to the 2-D model release scenarios except that the parcel density with respect to latitude is not weighted toward the higher latitude emission region as suggested by *Wuebbles et al.* [1993]. The release distribution also does not include the cross-equatorial emissions. The zonal symmetry of the release is justified by *Sparling et al.* [1995], who showed that a North Atlantic winter release rapidly becomes zonally symmetric; however, the main reason for such a simplified release scenario is to allow for clear interpretation of the results.

An instantaneous release is used so that the decay time can be unambiguously estimated. We have also performed one computationally intensive zonal release with 7380 parcels (E19M) to test the statistics of our release numbers. The computed global decay rates for E19M and E19 (Table 1) were found to be the same to within the uncertainty of the fit to the exponential tail. This indicates that the number of parcels used was sufficient to provide a statistically robust representation of the longest-lived eigenmode.

Every 10 days after the release the air parcels are checked to see if they have moved below the 250 hPa level, which is the approximate altitude of the midlatitude tropopause. Parcels found at altitudes below 250 hPa are assumed to be removed

by rainout. With this simple removal algorithm it is possible for parcels to enter the tropical troposphere from the midlatitude stratosphere and be relofted rather than be eliminated. In practice, this happens very rarely. Most parcels entering the tropical troposphere quickly follow isentropes to pressures above 250 hPa and are removed. A test of this removal algorithm against a more complex tropopause-following algorithm shows that this simple procedure gives virtually the same results as the more complex one.

Ten experiments are described below (Table 1). For each of the instantaneous aircraft exhaust releases, we start on January 2, 1994, and run the experiment until at least December 25, 1996. The experiment using the GEOS-STRAT winds begins on October 1, and the winds are recycled after the first year (i.e., the winds on October 1 are the same for each year of integration).

The first experiment, E19, is our base experiment, a 19 km release. This release corresponds to the maximum emission altitude of the combined HSCT (high-speed civil transport) fleet. The E19 altitude level includes potential temperature isopleths that are wholly in the stratospheric overworld. The E19M experiment is the 7380-parcel duplicate of E19 to test statistical robustness of E19. E19D is the same as E19, but uses the GEOS-STRAT winds and diabatic heating. E19C is a continuous release experiment to test the two different ways of computing lifetime. For E19C, parcels were added to the model over the E19 initialization domain at a rate of 648 parcels every 10 days. After about 2 years of integration, we developed a steady state of 22,000 parcels ± 1000, from which we computed the lifetime.

Experiment E190 is a repeat of E19, except the net heating rate is not globally balanced, which reduces the midlatitude net cooling rate and broadens the tropical net heating zone. As discussed above, the global-averaged net heating rate in the stratosphere should be close to zero [*Shine*, 1989; *Olaguer et al.*, 1992]. The fact that it is not close to zero suggests some uncertainty in the input parameters such as the temperature, the cloud fields, spectral parameters, or the ozone distribution. The intent of the E190 experiment is to give a general estimate as to the sensitivity of the results to uncertainties in the net heating rates.

Experiment E16 is a 16 km release to test the sensitivity of the results to initial altitude. This experiment straddles the overworld–middle world boundary. E13 and E14 correspond to 13 and 14 km releases, which would occur with a high-altitude subsonic aircraft. Like the E16 experiment the 14 and 13 km release altitudes includes a few potential temperature surfaces in the overworld. E11, at 11 km, corresponds to a subsonic effluent release which is entirely in the middle world.

The ^{14}C experiment is a bomb debris release to allow us to compare results with the 2-D and 3-D model bomb release studies [*Mahlman and Moxim*, 1978; *Johnston*, 1989; *NASA*, 1993]. The parcels are released at 520 K (about 22 km) from 20°N to 70°N. For this experiment the release begins in October 1992 [see *NASA*, 1993, Figure I-1a] and is run until December 15, 1996. A close examination of the trajectory model results suggests that a broad vertical distribution of parcels centered at 520 K should be used for this test case rather than the narrow-peaked altitude distribution used to initialize the integration. Thus we compare our results of the ^{14}C experiment to observations starting 1 year after initializing parcels on the 520 K surface.

3. Results

Plate 1 shows snapshots of the parcel distribution from the E19 experiment overlaid on the zonal mean net heating rate as a function of latitude and log pressure height. The zonal mean position of the tropopause and the 385 K potential temperature contour are also shown. The sequence in Plate 1 shows that one group of parcels disperse quickly out of the NH midlatitude region and into the tropics, while another group sinks into the middle world (between the dashed and solid lines in the plate). Parcels reaching the tropical stratosphere (or the region equatorward of about 30°N) are lofted by the diabatic heating. By July 1994, some parcels have moved through the tropics into the southern hemisphere (hereafter SH) or back into the NH at a higher potential temperatures than the initial release. The movement of parcels across the heating rate gradients effectively acts to produce a vertical dispersion of the parcels as discussed by *Sparling et al.* [1997]. After about 1.5 years the distribution of parcels becomes fairly uniform.

Figure 1 shows the time series of the number of parcels in different regions. The total number of parcels is initially constant, but this is followed by a rapid drop (delta) and then a steady exponential decay. This decay scenario is common to all the experiments and will be discussed further below. For E19 the time constant for the fit to the exponential decay tail is 1 year (Table 1). For the E19C experiment the lifetime is computed as 22,000 parcels/64.8 parcels per day giving a lifetime of 0.93 years. The slightly shorter lifetime E19C compared to E19 is expected since the E19C lifetime calculation includes the lifetime of the short-lived modes [*Prather*, 1996]. This result suggests that using the long-lived eigenmode for the lifetime estimate is equivalent to estimating the upper bound on the lifetime. For the E19D experiment (using the GEOS-STRAT assimilation winds) the lifetime is 1.2 years. All of these results are fairly close to the run-to–steady state 1.15 year lifetime estimate made by *Weaver et al.* [1996] using GEOS-1.

For all of the experiments except E11, the total parcel number curve can be divided into three segments: first, a period of no change in the total population; second, a period when the population drops rapidly (delta); and third, a period where the population drops more slowly but exponentially. Although parcels are dispersing during the first period, no change in the total population number occurs because none of the parcels has reached the 250 hPa sink region. The length of the "no change" time is directly proportional to the release altitude, since higher releases take longer to descend to 250 hPa. During the "no change" time segment, some parcels have descended to the middle world as a group. Once this group reaches the middle world, they are flushed from the middle world stratosphere within a month, which causes the rapid drop in parcel population (delta). The rapid flushing of the middle world is most clearly seen in the E11 experiment (Table 1) and occurs as a result of the strong eddy mixing of parcels along the middle world isentropes which bend below 250 hPa in the tropics. The magnitude of the delta tells us what percentage of parcels moved directly to the middle world and out of the stratosphere after their release.

The third stage is the slower exponential decay associated with the long-lived eigenmode. This is the stage where parcels have dispersed into the tropics and then into the southern hemisphere. These parcels eventually move out of the stratosphere when they reach the middle world.

The E16, E14, and E13 (Table 1) experiments give almost the same results as E19, except that the "no change" period is

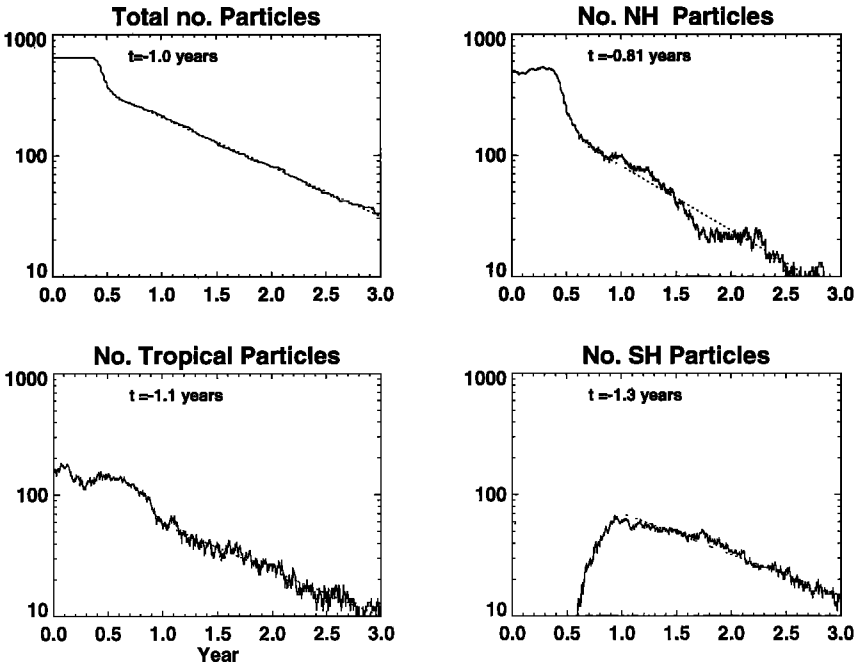

Figure 1. (top left) Total number of parcels verses year. The dotted line shows the fit to the line slope (over the region covered by the dotted line) with the timescale indicated. (top right) Parcel count in northern extratropics (30°N to the pole) and the corresponding fit. (bottom left) Tropical parcel count (30°S to 30°N). (bottom right) Southern extratropical parcel count (30°S to the pole).

shorter, and the population drop is larger because the parcels are released closer to the middle world. The ^{14}C experiment also gives similar results, except that the decay time is 1.3 years because the higher altitude of the release gives the parcels more time to disperse globally, which appears to slightly increase the lifetime. The increase in tracer lifetime with release altitude was also noted by *Mahlman and Moxim* [1978].

In all but the E11 experiment, some parcels are released into the overworld, and thus parcels can mix to the tropics to be lofted. The E11 release takes place entirely in the middle world. For the E11 case the removal level is lowered to 350 hPa, which is just below the tropopause. All of the exhaust is removed within 2 months; the computed lifetime is about 0.5 months. The E11 experiment was also performed for NH summer with similar lifetime results.

It is interesting to look at the lifetime of parcels in different latitude regions as shown in Figure 1. We have divided the domain into northern hemisphere (30°N to 90°N), southern hemisphere (30°S to 90°S) and tropics (30°S to 30°N). The definition of the tropical boundary is somewhat arbitrary; the results are generally the same if the boundary is chosen to be 20°. In the NH the lifetime is shorter (about 0.8 years), while the lifetimes in the tropics and the SH are longer. Note that it takes about 1 year for the SH to fill with parcels and then begin to decay.

Figure 2 shows the flux and tendency of parcels for the tropical (equatorward of 30°) and extratropical and regions for the E19 case. In the NH the dominant loss is to the troposphere (negative tropospheric source). There is also an initial NH extratropical gain from the tropics, since some of the parcels are initialized equatorward of 30°N. After about 0.2 years, however, NH parcels are moving into the tropics on average. For the SH the tropics is a source of parcels, which after some transience is balanced by the tropospheric sink.

The tropical fluxes are complicated. Initially, some tropical parcels move to the NH, generating a negative net tendency. This flux reverses after 0.2 years, and parcels flow from the NH to the tropics and are lost. This should not be interpreted as descent out to the equatorial tropical stratosphere; rather it is removal of formerly midlatitude stratospheric parcels which have moved along isentropes into the tropical upper troposphere. Note that the jump in tropical tropospheric parcel loss exactly corresponds to the E19 delta shown in Figure 1. There is no evidence of downward vertical transport in the equatorial tropical stratosphere as was reported by *Weaver et al.* [1996]. Their result implies that there must be sufficient vertical diffusion to overwhelm the upward advection. Recent experiments with the chemical transport model used by Weaver et al. suggest that the assimilation kinematic vertical velocities may generate excessive diffusion (S. Strahan, personal communication, 1997).

We have run a comparison of the equivalent E19 experiment with the GSFC 2-D model [e.g., *Jackman et al.*, 1996] as shown in Plate 2. A similar 2-D/3-D model comparison was performed by *Weaver et al.* [1996] and *Rasch et al.* [1994] for shorter periods. None of the 2-D models used in these studies nor the one used here have circulations identical to the 3-D calculation, so only the broadest conclusions can be derived from the intercomparisons.

Since the density of the parcel distribution corresponds to a constituent number density, we can convert the distribution of air parcels to mixing ratio assuming that the number of parcels within an averaging volume is statistically significant. The E19 mixing ratio is computed by counting parcels within a 2 km by 10° latitude grid, dividing by the atmospheric number density, and normalizing to the 2-D model initial mixing ratio. The resolution of the 2-D model is also 2 km by 10° latitude with the model points offset from the parcel averaging grid by 5°.

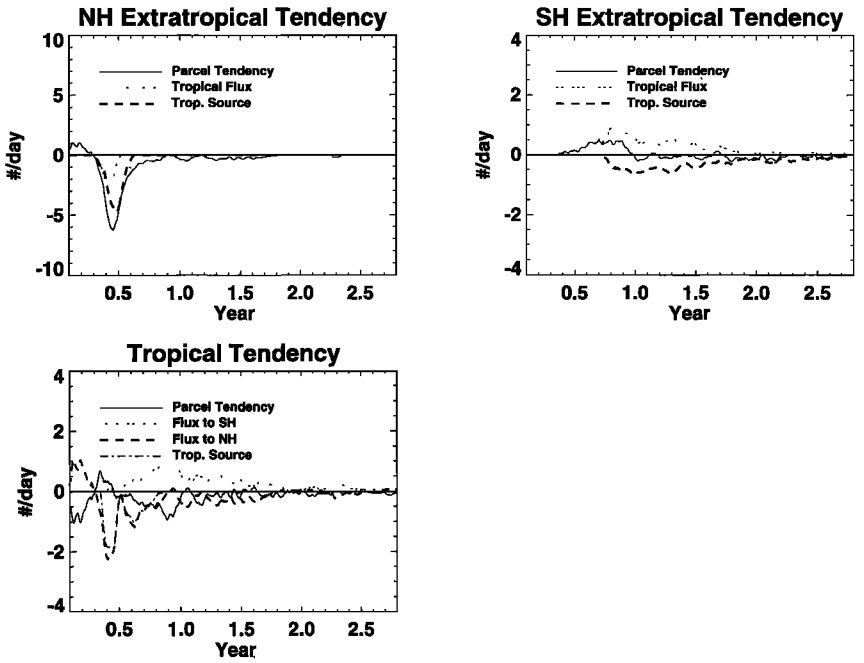

Figure 2. Tendencies and fluxes for E19. The fluxes between the NH, SH, and tropical regions are as indicated. "Trop. source" means source from the troposphere. A negative value means a sink. The tendency term is the time derivative of the number of parcels in each of the regions. The data in Figure 1 were smoothed with a weak box car filter over the whole period before the tendencies were computed.

The tracer is initialized in the same height and latitude region as the 2-D model. The 2-D model tracer is also eliminated below 250 hPa as were the trajectory parcels. The computed lifetime for the 2-D model tracer in this experiment is 1.5 years, which is slightly shorter than the 1.7 year lifetime [*NASA*, 1993] computed using an earlier dynamical formulation.

Plate 2 shows that both the 2-D and trajectory models are in good agreement up to about 100 days. Subsequently, the 2-D model tracer is more confined to the northern hemisphere and retains a high mixing ratio in the middle world. The more rapid dispersal of the tracer by the trajectory model into the tropics and then to the southern hemisphere is consistent with the results from *Rasch et al.* [1994]. After roughly 2 years, the 2-D model tracer has reached high altitudes, but is still mostly confined to the northern hemisphere. In contrast, the E19 mixing ratio is highest in the southern hemisphere.

Figure 3 shows the results of the ^{14}C experiment which corresponds to Figure I-2 of *NASA* [1993]. The parcel distribution (after 1 year) is converted to a mixing ratio using the initial ^{14}C observations. Consistent with observations, the model retains a ^{14}C peak at about 20 km, and this peak ascends with time. The magnitude of the peak initially decays at about the same rate as the observations, although after 2 years there are too few parcels to make the comparison very meaningful (Figure 3, lower right). Also note that the dynamics for 1963–1965 is different than the period 1993–1995. Our lifetime estimate of 1.3 years is shorter than the 2 year ^{14}C asymptotic lifetime estimates of *Mahlman and Moxim* [1978]. Observations show that the ^{14}C residence time varies from about 1.5 to 2 years [*Fabian and Libby*, 1974]. The shorter decay time in the trajectory model appears to be due to the more rapid interhemispheric exchange when the trajectory results are compared with the *Mahlman and Moxim* [1978] simulations.

The final experiment is E190, in which the global cooling rates are not balanced. This experiment tests the sensitivity of our results the changes in the net heating. Plate 3 shows the change in the annual mean net heating rate as a result of rebalancing the heating rates. The most significant change is the increased midlatitude cooling and the reduced tropical heating which occurs after rebalancing. The net result is that the lifetime of the tracer is comparatively longer for the unbalanced heating rates because of the weaker midlatitude net cooling. We consider the difference in the lifetimes for the E19 and E190 experiments, 0.6 years, to be an upper bound on the estimate of the uncertainty in the effluent lifetime.

4. Summary and Conclusions

A series of 3-year integrations of a diabatic trajectory model is used to study the lifetime of instantaneous, northern hemisphere, aircraft effluent releases at a variety of altitudes. Most of the experiments are performed using UKMO assimilated wind fields for horizontal transport. Cross-isentropic motion is calculated for globally balanced net heating rates derived from the UKMO temperature and climatological ozone and cloud fields. Parcels descending below 250 hPa are assumed to be in the troposphere and are removed. To check on the sensitivity of the simulations to wind fields, one experiment was performed with GEOS-STRAT assimilated winds and diabatic heating rates. The GEOS-STRAT experiments gave a slightly longer lifetime. Statistical robustness of the model was tested by increasing the parcel number by a factor of more than 10, and the model performance was also checked by simulating ^{14}C bomb debris data from the late 1960s. Both tests indicated that there were no simulation anomalies.

The effluent release lifetime is computed using a fit to the exponential tail of the parcel number time series. This is equivalent to computing the decay time of the long-lived eigenmode

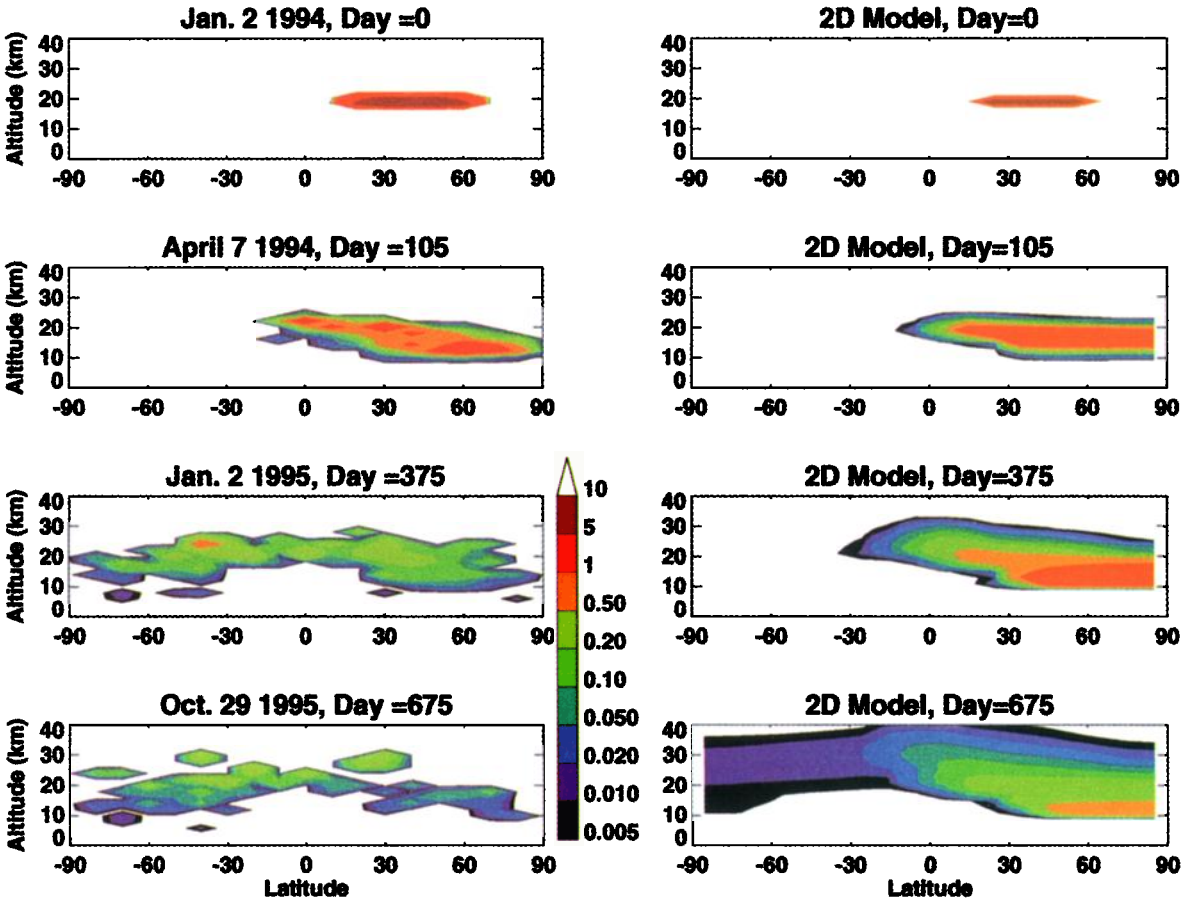

Plate 2. Comparison of trajectory model and 2-D model results for the E19 experiment. E19 results are shown as mixing ratio by averaging parcels in 2 km by 10° and computing the mixing ratio. The tracer has arbitrary units; color scaling is indicated in the colored boxes.

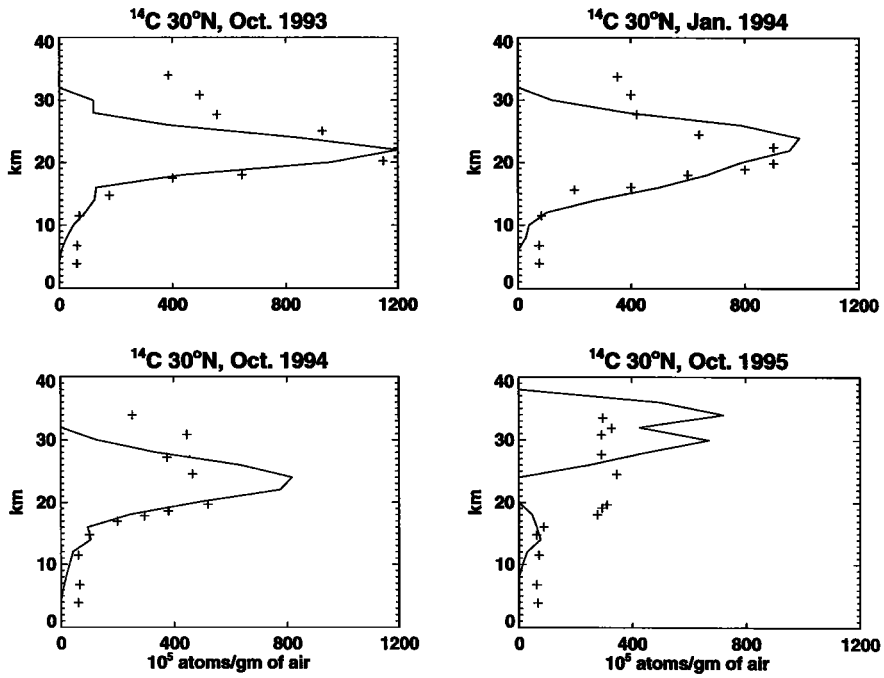

Figure 3. Model mixing ratio profiles for ^{14}C (solid line) and data (pluses) [after *NASA*, 1993, Figure I-2].

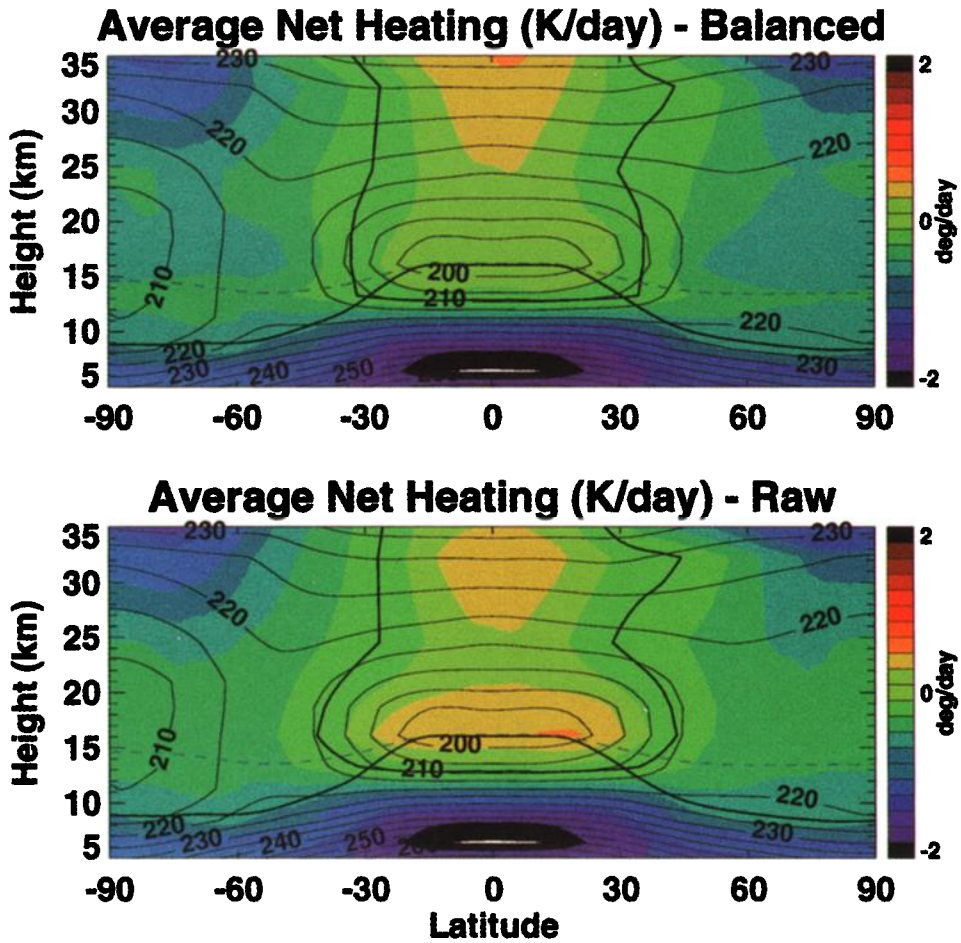

Plate 3. The annual average net heating rate in K/day for 1994. Black contours show annual mean temperature from UKMO assimilation. (top) Heating rates after the global mean net heating along each pressure surface has been subtracted. (bottom) Heating rates without adjustment.

[*Prather*, 1996], which will not be the same as a run-to–steady state computed lifetime, because the steady state lifetime includes the effect of all eigenmodes. To check whether the shorter-lived modes were important, we also performed a continuous release test and computed the run-to–steady state lifetime. The slightly shorter lifetime of this experiment (0.84 years compared to 1 year) suggests that the our computed lifetimes should be considered upper bounds on the steady state lifetime.

We find that the global lifetime for effluents released at 19, 16, 14, and 13 km in the NH stratosphere is slightly more than 1 year, with the lifetime slightly increasing with release altitude. The lifetime increase with altitude, also reported by *Mahlman and Moxim* [1978], is expected since higher released parcels will have more opportunity to mix into the tropics and be lofted, decreasing their probability of exiting the stratosphere. It also suggests that an even longer-lived eigenmode may be excited by the higher-altitude release.

Except for the 11 km release, there are three clear time regimes for the global parcel evolution. First, there is a short period of no change which is followed by the second period where there is a rapid drop (or delta) in parcel count. During the first period, most of the parcels are descending in the NH from the overworld to the middle world. Some parcels are also dispersing into the tropics. The higher the release, the more parcels disperse into the tropics during this phase. The rapid drop in the second period occurs as the large group of parcels reach the NH middle world and are quickly flushed from the stratosphere. The parcels dispersed to the tropics are lofted by the net diabatic heating. These parcels begin a complex life history, often ascending and descending many times again as they move in and out of the tropical net heating region. Eventually, these parcels find their way to the middle world and are flushed out of the stratosphere. This leads to the third regime, a slow exponential decay in the parcel count.

The ability of the middle world to flush material rapidly out of the stratosphere is demonstrated by our 11 km release, which takes place entirely within the middle world. The parcels quickly exit the lower stratosphere with a lifetime of about 0.5 months. The middle world ventilation takes place mostly through isentropic, cross-tropopause mixing between the tropics and midlatitudes [e.g., *Dessler et al.*, 1995]. In general, we find that unless parcels are released above 385 K the lifetime is less than a month. The highest-altitude subsonic commercial aircraft can reach about 13 km. At that altitude a very small fraction (less than 5%) of the effluent is released at 385 K or above.

We have also found that the lifetime of parcels in the SH is slightly longer than the lifetime in the NH. The asymmetry in hemispheric lifetime is also seen in the National Center for Atmospheric Research (NCAR) 3-D model lifetime experiment [*Hall and Waugh*, 1997]. The asymmetric lifetime is due

to the comparatively colder SH stratosphere, which results in lower net diabatic cooling rates and a weaker flushing of the lower midlatitude stratosphere (see Plate 3). The lower eddy amplitudes in the SH [see *Randel*, 1992] are, no doubt, responsible for the weaker diabatic circulation.

The trajectory model effluent lifetime of 1–1.2 years (E19, E19M, E19D) is generally consistent with the *Weaver et al.* [1996] 3-D model estimates of 1.15 years, but shorter than the GSFC 2-D model estimate of 1.5 years for the E19 experiment. Comparisons with the 2-D model show that the 3-D calculation produces more cross-hemispheric exchange and ventilates the middle world faster than the 2-D model.

Finally, the lifetime for the E19 release is quite sensitive to the net heating rate. If the heating rates are not globally balanced, then the lifetime increases to 1.5 years (E190). Globally balancing the heating rates is functionally equivalent to making the global-averaged residual vertical velocity equal to zero for the stratosphere, which is assumed for most 2-D models. To make the global-averaged net diabatic heating rates sum to zero, the residual is evenly subtracted at each latitude (uniform balancing). In our case, uniform balancing increases the midlatitude cooling rate and shortens the lifetime. Since the globally balanced net heating fields also produce reasonable 2-D model simulations of column ozone and the distribution of other trace gases, the most we can conclude is that uncertainty in the net diabatic heating rate creates some uncertainty in the global effluent lifetime, but this uncertainty is probably not as large as the difference between the balanced and the unbalanced net heating rate fields.

Acknowledgments. We would like to thank the reviewers and Anne R. Douglass for helpful comments on the manuscript, and O. Brian Toon for suggesting the ^{14}C simulations. Michael Prather pointed out the eigenmode interpretation of the lifetime. This work was supported by the EOS interdisciplinary Science Program and the Atmospheric Effects of Aviation Program.

References

Avallone, L. M., and M. J. Prather, Photochemical evolution of ozone in the lower tropical stratosphere, *J. Geophys. Res.*, *101*, 1457–1461, 1996.

Dessler, A. E., E. J. Hintsa, E. M. Weinstock, J. G. Anderson, and K. R. Chan, Mechanisms controlling water vapor in the lower stratosphere: "A tale of two stratospheres," *J. Geophys. Res.*, *100*, 23,167–23,172, 1995.

Douglass, A. R., C. J. Weaver, R. B. Rood, and L. Coy, A three-dimensional simulation of the ozone annual cycle using winds from a data assimilation system, *J. Geophys. Res.*, *101*, 1463–1474, 1996.

Fabian, P., and W. F. Libby, The stratospheric residence time of odd nitrogen and the effect of the SST studied in a two-dimensional model derived from high-altitude sampling of radioactive debris, in *Proceedings, Third Conference of the Climatic Impact Assessment Program*, edited by A. J. Broderick and T. M. Hard, *TSC-OST-74-15*, pp. 103–116, Dep. of Transp., 1974.

Hall, T., and D. Waugh, Timescales for the stratospheric circulation derived from tracers, *J. Geophys. Res.*, *102*, 8991–9001, 1997.

Holton, J. R., P. H. Haynes, M. E. McIntyre, A. R. Douglass, R. B. Rood, and L. Pfister, Stratosphere-troposphere exchange, *Rev. Geophys.*, *33*, 403–439, 1995.

Jackman, C. H., E. L. Fleming, S. Chandra, D. B. Considine, and J. E. Rosenfield, Past, present and future modeled ozone trends with comparisons to observed trends, *J. Geophys. Res.*, *101*, 28,753–28,767, 1996.

Johnston, H. S., Evaluation of excess carbon 14 and strontium 90 data for suitability to test two-dimensional stratospheric models, *J. Geophys. Res.*, *94*, 18,485–18,493, 1989.

Mahlman, J. D., and W. J. Moxim, Tracer simulation using a global general circulation model: Results from a midlatitude instantaneous source experiment, *J. Atmos. Sci.*, *35*, 1340–1374, 1978.

Minschwaner, K., A. E. Dessler, J. W. Elkins, C. M. Volk, D. W. Fahey, M. Loewenstein, J. R. Podolske, A. E. Roche, and K. R. Chan, The bulk properties of isentropic mixing into the tropics in the lower stratosphere, *J. Geophys. Res.*, *101*, 9433–9439, 1996.

Murgatroyd, R. J., and F. Singleton, Possible meridional circulations in the stratosphere and mesosphere, *Q. J. R. Meteorol. Soc.*, *87*, 125–135, 1961.

NASA, The Atmospheric Effects of Stratospheric Aircraft: Report of the 1992 Models and Measurements Workshop, *NASA Ref. Publ. 1292*, 352 pp., 1993.

NASA, Scientific Assessment of the Atmospheric Effects of Stratospheric Aircraft, *NASA Ref. Publ. 1381*, 64 pp., 1995.

Olaguer, E. P., H. Yang, and K. K. Tung, A reexamination of the radiative balance in the stratosphere, *J. Atmos. Sci.*, *49*, 1242–1263, 1992.

Plumb, R. A., A "tropical pipe" model of stratospheric transport, *J. Geophys. Res.*, *101*, 3957–3972, 1996.

Prather, M. J., Timescales in atmospheric chemistry: Theory, GWPs for CH_4 and CO, and runaway growth, *Geophys. Res. Lett.*, *23*, 2597–2600, 1996.

Randel, W. J., Global atmospheric circulation statistics, 1000–1 mb, *NCAR Tech. Note TN-366+STR*, 256 pp., Natl. Cent. for Atmos. Res., Boulder Colo., 1992.

Rasch, P. J., X. Tie, B. A. Boville, and D. L. Williamson, A three-dimensional transport model for the middle atmosphere, *J. Geophys. Res.*, *99*, 999–1017, 1994.

Rood, R. B., A. R. Douglass, M. C. Cerniglia, and W. G. Read, Synoptic-scale mass exchange from the troposphere to the stratosphere, *J. Geophys. Res.*, *102*, 23,467–23,485, 1997.

Rosenfield, J. E., P. A. Newman, and M. R. Schoeberl, Computations of diabatic descent in the stratospheric polar vortex, *J. Geophys. Res.*, *99*, 16,677–16,689, 1994.

Rosenfield, J. E., D. B. Considine, P. E. Meade, J. T. Bacmeister, C. H. Jackman, and M. R. Schoeberl, Stratospheric effects of the Mt. Pinatubo aerosol studied with a coupled two-dimensional model, *J. Geophys. Res.*, *102*, 3649–3670, 1997.

Schoeberl, M. R., and L. Sparling, Trajectory modeling, in Diagnostic Tools in Atmospheric Physics, edited by G. Fiocco and G. Visconti, *Proc. Int Sch. Phys. Enrico Fermi*, *124*, 289–306, 1995.

Schoeberl, M. R., et al., An estimation of the dynamical isolation of the tropical lower stratosphere using UARS wind and trace gas observations of the quasi-biennial oscillation, *Geophys. Res. Lett.*, *24*, 53–56, 1997.

Shine, K., Sources and sinks of zonal momentum in the middle atmosphere diagnosed using the diabatic circulation, *Q. J. R. Meteorol. Soc.*, *115*, 265–292, 1989.

Sparling, L. C., M. R. Schoeberl, A. R. Douglass, C. J. Weaver, P. A. Newman, and L. R. Lait, Trajectory modeling of emissions from lower stratospheric aircraft, *J. Geophys. Res.*, *100*, 1427–1438, 1995.

Sparling, L. C., J. A. Kettleborough, P. H. Haynes, M. E. McIntyre, J. E. Rosenfield, M. R. Schoeberl, and P. A. Newman, Diabatic cross-isentropic dispersion in the lower stratosphere, *J. Geophys. Res.*, *102*, 25,817–25,829, 1997.

Swinbank, R., and A. O'Neill, A stratosphere-troposphere data assimilation system, *Mon. Weather Rev.*, *122*, 686–702, 1994a.

Swinbank, R., and A. O'Neill, Quasi-biennial and semi-annual oscillations in equatorial wind fields constructed by data assimilation, *Geophys. Res. Lett.*, *21*, 2099–2102, 1994b.

Volk, C. M., et al., Quantifying transport between the tropical and mid-latitude stratosphere, *Science*, *272*, 1763–1768, 1996.

Weaver, C. J., A. R. Douglass, and D. B. Considine, A 5-year simulation of supersonic emission transport using a three-dimensional model, *J. Geophys. Res.*, *101*, 20,975–20,984, 1996.

Wuebbles, D. J., et al., Emission scenarios development: Report of the emissions scenarios committee, in *The Atmospheric Effects of Stratospheric Aircraft: Third Program Report*, edited by R. Stolarski and H. L. Wesoky, chap. 3, *NASA Ref. Publ.*, *1313*, 63–208, 1993.

C. H. Jackman and M. R. Schoeberl, NASA Goddard Space Flight Center, Code 910, Greenbelt Road, Greenbelt, MD 20771-0001. (e-mail: schom@zephyr.gsfc.nasa.gov)

J. E. Rosenfield, General Sciences Corporation, 6100 Chevy Chase Drive, Laurel, MD 20810.

(Received May 21, 1997; revised January 26, 1998;
accepted January 27, 1998.)